2022-01-0678 Published 29 Mar 2022

Chevrolet Bolt Electric Vehicle Model Validated with On-the-Road Data and Applied to Estimating the Benefits of a Multi-Speed Gearbox

Fabricio Machado, Phillip Kollmeyer, and Ali Emadi McMaster University

Citation: Machado, F., Kollmeyer, P., and Emadi, A., "Chevrolet Bolt Electric Vehicle Model Validated with On-the-Road Data and Applied to Estimating the Benefits of a Multi-Speed Gearbox," SAE Technical Paper 2022-01-0678, 2022, doi:10.4271/2022-01-0678.

Received: 24 Jan 2022 Revised: 24 Jan 2022 Accepted: 10 Jan 2022

Abstract

This paper presents a model for predicting the energy consumption of a 2017 Chevrolet Bolt electric vehicle. The model is validated using 93 measured drive cycles covering in excess of 10,600 kilometres of driving and temperatures from −8 to 32 °C. The mechanical road load acting on the vehicle is calculated via ABC parameters from the publicly available US Environmental Protection Agency (EPA) Annual Certification Data database. The vehicle model includes wheel diameter, gear ratio, rated electric machine torque and power, 12V accessory load based off measurements, measured electric machine efficiency obtained from a publication from General Motors, and modelled inverter efficiency. Assumptions are made regarding gearbox losses as well. To ensure accuracy under real-world conditions, road grade, temperature effects, and heating and cooling energy are included as well. The model predicts an EPA range of 380 km, which is very close to the 383 km rating. Error is typically around ±10% for the experimental drive cycles used for validation. The presented modelling methodology can be applied to any production battery electric vehicle and used to predict the benefits of utilizing multi-speed gearboxes, wideband gap semiconductor inverters, different electric traction machine designs, and other vehicle design changes. The paper includes an extensive comparison of modelled versus measured results, as well as an analysis of the benefits of a multi-speed gearbox for the vehicle, showing an increase of range of 1.3% (5 km) with a two-speed gearbox.

Introduction

Global warming has forced the automotive industry to drastically decrease vehicle emissions towards zero CO_2. Over twenty countries have announced ambitious goals to reduce vehicular greenhouse gas emissions by restricting or even banning the selling of internal combustion engine (ICE) propelled vehicles. For example, the United Kingdom will ban ICE-propelled vehicles in 2030, followed by Japan and China in 2035 [1]. To achieve these challenging targets, automakers such as General Motors (GM) have been heavily investing in vehicle electrification and setting public commitments to offer new global, fully electrified products in a short period. GM, for example, plans to invest 35 billion dollars in expanding its portfolio to 30 new battery electric vehicles (EV) by 2025 [2] and even has a notable plan to produce only zero-emission vehicles by 2035 [3].

Nevertheless, the vehicle powertrain design process is complex. To manage this complexity, a new system development framework is proposed in [4], where model-based design is used to support the system requirements, design, analysis, verification, and validation activities. Thus, this paper presents the performance of a straightforward way to model an electromechanical EV powertrain that incorporates the electric machine, inverter, gearbox and differential, and the mechanical forces acting on the vehicle, including the aero drag force, acceleration force, rolling resistance force, and gravitational incline force. These mechanical forces contrapose the vehicle's movement and are used to calculate the power demand from the high-voltage battery. The model is used to estimate the vehicle energy consumption, predicted electric machine and inverter efficiencies, and the distribution of the system energy. The model is also used to predict the benefits of a two-speed gearbox and its impact on vehicle energy consumption. Other vehicle powertrain configurations can be further incorporated, for instance, wideband gap semiconductor inverters, different electric traction machine designs, and other powertrain changes. The model is based on backwards power losses equations, having as input the required vehicle speed, and is demonstrated for the 2017 Chevrolet Bolt EV as a benchmark.

Vehicle modelling has been extensively detailed in the literature, and various authors have proposed different modelling approaches to predict the power and energy required for a given drive cycle. In [5], the MATLAB/Simulink Powertrain Blockset™ is applied towards the design of a hybrid vehicle

TABLE 1 2017 Chevrolet Bolt EV data logging measured parameters.

Parameter	Symbol	Unit
Time Step	t	s
Air Conditioning Power	P_{air_cond}	W
Heater Power	P_{heater}	W
High-Voltage Battery Current	I_{batt}	A
High-Voltage Battery Voltage	V_{batt}	V
High-Voltage Battery State-of-Charge	SOC	SOC
Latitude	Lat	degrees
Longitude	$Long$	degrees
Outside Air Temperature	T	Celsius
Odometer	Odo	km
Vehicle Speed	v_{veh}	m/s

TABLE 2 2017 Chevrolet Bolt EV model parameters.

Vehicle Parameter	Symbol	Value	Unit
Vehicle Mass Unloaded	m_{veh}	1625	kg
Vehicle Load (driver)	m_{load}	80	kg
A factor	A	126.3295	N
B factor	B	2.0079	N/(m/s)
C factor	C	0.4207	N/(m/s)^2
Final Gear Ratio	G_f	7.05	-
Wheel Radius (215/50 R17 tire)	r_{wh}	0.323	m

TABLE 3 Chevrolet Bolt EV electric machine parameters [13].

Parameter	Value	Unit
Peak power	150	kW
Peak torque	360	Nm
Max speed	8810	RPM
Peak power density	28.8	kW/litre
Peak torque density	70	Nm/litre
Rated current	400	Arms
Nominal DC bus voltage	350	V

TABLE 4 Chevrolet Bolt EV cumulative measured performance.

Parameter	Measurement	Unit
Number of Drives	93	N/A
Total Distance	10,656	km
Average Trip Distance	114.7	km
Total Trip Time	152.7	hour
Average Driving Speed	70	Km/h
Maximum Driving Speed	124	Km/h
Typical 12V Accessory Power	200	W
Average Heater Power[1]	2.1	kW
Average Air Conditioning Power[1]	0.73	kW
Total Heater Energy Consumed	195.2	kWh
Total Air Conditioning Energy Consumed	22.4	kWh
Total Battery Discharge Energy	1912.7	kWh
Average Battery Discharge Energy	179.5	Wh/km
Total Battery Discharge Energy (due to motoring)	2,071.6	kWh
Average Battery Discharging Energy (due to motoring)	194.4	Wh/km
Total Battery Charge Energy (due to regenerative braking)	–158.8	kWh
Average Battery Charge Energy (due to regenerative braking)	–14.9	Wh/km

[1] While on

drivetrain. In [6], NREL's Advanced Vehicle Simulator, ADVISOR, is used to model a vehicle and create a machine learning battery state-of-charge (SOC) estimation algorithm for the modeled vehicle. An electric vehicle design process, in which constant electric machine and drive efficiency were assumed, was developed in MATLAB in [7] and used to predict energy consumption in different scenarios. To validate their model, the author simulated the range of a Nissan Leaf EV and compared it with the Environmental Protection Agency (EPA) rated driving range, finding less than 5% difference in driving range.

An electromechanical modelling approach for an EV is showcased in [8] for a 3-wheeled Corbin Sparrow EV, which was produced in the early 2000s. This model is validated with on-the-road data, totaling a driving distance of nearly 500 km, for which an average model error of 7.5% was observed [9]. In [10], a Ford F150 truck is retrofitted into an EV. The truck is heavily instrumented with sensors for data acquisition, including a torque sensor embedded in the driveline. A sophisticated model of the truck, including all the electromechanical drivetrain components, was created and validated for 500 km of driving data. Model error was found to be within +/- 10% except for drives with significant headwinds, where the error was as high as 24% [11]. A comprehensive model of a Ford Focus EV was created in [12] using experimental test data collected on a vehicle dynamometer. After performing several different drive cycle measurements with the dynamometer, the model was found to accurately predict the energy consumption with a very low error of just 4.2%.

While the modeling approach proposed in this paper is similar to previously presented vehicle models, this work has a couple of aspects which set it apart from, such as the inclusion of the effect of temperature on aerodynamic drag, the analysis of model error for a wide range of temperatures, and the investigation of heating and cooling loads on vehicle energy consumption. More than 90 recorded drive trips, primarily travelling from Buffalo-NY to Hamilton-ON and vice-versa, covering over 10,600 kilometres of driving, were used to validate the model. The model also integrates the road grade variation and the effect of outside air temperature, ranging from –8 to 32 °C, on energy consumption. The heater and air conditioner measured power are also included to ensure accuracy under real conditions. The model is also primarily populated with parameters which are publicly available for any production vehicle, so it can easily be recreated and used for other vehicle types. Specifically, the model parameters include vehicle mass, load mass, ABC road load parameters, gear ratio, and wheel radius, as are all listed in Table 2, average 12V accessory power as listed in Table 4, as well as inverter and traction machine efficiency maps.

If inverter and traction machine efficiency maps are not available, a fixed efficiency value for each could be assumed instead.

The paper is organized as follows: vehicle modelling methodology and data logging, including the vehicle logged parameters, mechanical and electromechanical model. Subsequently, the analysis of drive data logged with the vehicle is presented, followed by the model-predicted division of energy consumption for logged drives and the model performance and accuracy for EPA range calculation and for logged drives. Finally, the model predicted benefits of a two-speed gearbox is exhibited.

Vehicle Modelling Methodology and Data Logging

In order to accelerate a vehicle, the powertrain must provide sufficient torque to overcome the mechanical forces acting on the vehicle. The aero drag force, acceleration force, rolling resistance force, and gravitational incline force oppose the vehicle movement, and therefore, the electric machine developed force must be higher than those forces to accelerate the vehicle, as shown in Figure 1. The road loads (F_{drag} or P_{drag}) are comprised of the electric machine friction and windage torque (1), gearbox and differential friction torque (2), bearings and tires friction torque (2), and the aero drag force (F_{aero}).

At any given time, the forces on the vehicle must be balanced, meaning that the electric machine mechanical force or power ($\boldsymbol{P_{em\_mech}}$) must be equal to the mechanical force or power acting on the vehicle ($\boldsymbol{P_{mech}}$). The power of the mechanical forces comprises of the sum of the acceleration power ($\boldsymbol{P_{accel}}$), gravitational incline power ($\boldsymbol{P_{grav}}$) and total drag power ($\boldsymbol{P_{drag}}$), as expressed in equation (1). When the vehicle is cruising at a constant speed, and on a flat road, the acceleration power and gravitational incline power are zero.

$$P_{em\_mech} = P_{mech} = P_{accel} + P_{grav} + P_{drag} \tag{1}$$

The high-voltage battery must supply the electric machine mechanical power, as well as the electric machine loss ($\boldsymbol{P_{em\_loss}}$), the inverter motor controller loss ($\boldsymbol{P_{inv\_loss}}$), and the accessory power ($\boldsymbol{P_{acc}}$). The heater power ($\boldsymbol{P_{heater}}$) and air conditioning power ($\boldsymbol{P_{air\_cond}}$) must also be supplied by the high-voltage battery, so battery power ($\boldsymbol{P_{batt}}$) can be expressed as:

$$\boldsymbol{P_{batt}} = \boldsymbol{P_{em\_mech}} + \boldsymbol{P_{em\_loss}} + \boldsymbol{P_{inv\_loss}} + \boldsymbol{P_{acc}} + \boldsymbol{P_{heater}} + \boldsymbol{P_{air\_cond}} \tag{2}$$

FIGURE 1 Overview of the mechanical forces acting on the vehicle contraposing the movement.

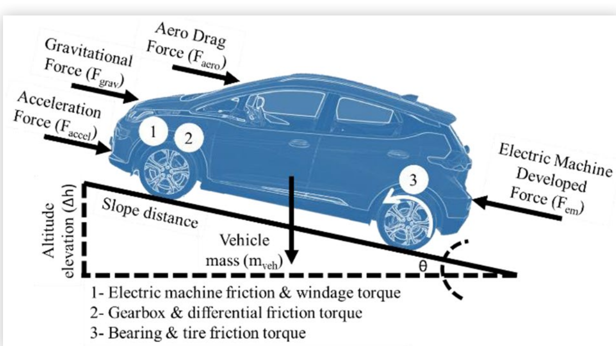

Vehicle Data Logged Parameters

The Chevrolet Bolt EV data was recorded by a module sold by Fleetcarma™, which utilizes the onboard vehicle diagnosis (OBDII) port as a connection to the diagnosis system of the vehicle. This device provides the ability of diagnostic scanning as well as to plot data stored on the internal communication network of the vehicle from the CAN bus. For the vehicle modelling, each measured signal is filtered to a bandwidth of 1 Hz. The raw data recorded by the OBDII device are exhibited in Table 1.

Mechanical Model

The total mechanical power forces acting on the vehicle consist of three components expressed in equation (3).

$$P_{mech} = P_{accel} + P_{grav} + P_{drag} \tag{3}$$

where P_{accel} is the acceleration power, P_{grav} is the power required to overcome the gravitational forces on an incline, and P_{drag} comprises the sum of the rolling resistance, aerodynamic drag, and other frictional forces acting on the vehicle. To calculate these power values and the resulting traction machine torque, only a few basic parameters are needed, all of which are listed in Table 2 and which can be gotten from publicly available sources for any vehicle produced in the US.

The vehicle mass, m_{veh}, and final gear ratio, G_f are all typically stated by the vehicle manufacturer, and for the Chevrolet Bolt EV are listed in [13] The wheel radius, r_{wh}, is shown in [14]. The ABC road load parameters used to calculate P_{drag} are available in the US Environmental Protection Agency's (EPA) Annual Certification Data database [15]. The parameters for all production vehicles sold in the US are determined in accordance with the SAE J1263 road load test standard [16]. Because the Chevrolet Bolt EV does not have a clutch to disengage the gearbox and differential from the electric machine while performing the coast down test to measure the road load parameters, it is assumed that the gearbox and differential losses are included in the losses captured by the ABC parameters. Table 2 summarizes the primary vehicle parameters.

The technique for calculating each power component as a function of the measured parameters and the vehicle's linear velocity, vertical velocity, and linear acceleration are discussed in the following subsections.

Vehicle Equivalent Mass due to Rotational Inertia The Chevrolet Bolt EV has a two-stage single-speed gearbox connecting the electric machine to the differential and front wheels [13]. The rotating component mass affects the vehicle acceleration, and their equivalent mass reflected the linear motion frame is a function of the rotational inertia of the component (J_{comp}), the operational gear ratio between that component and the wheel (*GR*), and the radius of the wheel (r_{wh}), as expressed in equation 4:

$$m_{eq} = J_{comp}\left(\frac{GR}{r_{wh}}\right)^2 \tag{4}$$

For a complete derivation and description regarding equation (4), see [11]. The equivalent mass must be calculated for each rotating component, followed by the total vehicle equivalent mass, as presented in equations 5 and 6, respectively.

$$m_{veh\_total} = m_{veh} + m_{load} \tag{5}$$

$$m_{veh\_eq} = m_{veh\_total} + m_{J\_em\_eq} + m_{J\_gearbox\_eq} + m_{J\_diff\_eq} + 4m_{J\_wh\_eq} \tag{6}$$

where m_{veh_eq} is the vehicle equivalent mass, $m_{J\_em\_eq}$ is the electric machine equivalent mass, $m_{J\_gearbox\_eq}$ is the gearbox equivalent mass, $m_{J\_diff\_eq}$ is the differential equivalent mass, and $m_{J\_wh\_eq}$ is each wheel's equivalent mass. All units are in kg.

Nevertheless, the majority of these inertial parameters are not publicly available unless a vehicle teardown is performed and measurements of each component are taken, which was outside the scope of this work. Therefore, a total vehicle equivalent mass was assumed to be 3% of the total vehicle mass, which is equal to that calculated for the electric truck in [10] operating in second gear.

Acceleration Power In order to linearly accelerate the total mass of the vehicle and to rotationally accelerate the inertia of the rotating components, a force must be applied. The vehicle acceleration (a_{veh}) is calculated by differentiating the measured vehicle speed (v_{veh}), in accordance with equation (7), where at each time step *k* acceleration is calculated based on the velocity at the next and previous time step to ensure the conservation of energy throughout the drive cycles. Subsequently, the calculated acceleration and vehicle equivalent mass (m_{veh_eq}) are used to determine the force (F_{accel}) and power (P_{accel}) required to accelerate the vehicle, as per equations (8) and (9), respectively.

$$a_{veh} = \frac{dv_{veh}}{dt} \approx \frac{v_{veh}(k+1) - v_{veh}(k-1)}{2\Delta t} \tag{7}$$

$$F_{accel} = m_{veh\_eq}\, a_{veh} \tag{8}$$

$$P_{accel} = m_{veh\_eq}\, a_{veh}\, v_{veh} \tag{9}$$

Gravitational Incline Power The gravitational incline power is the required power to overcome a slope when the vehicle is moving uphill. Conversely, the gravitational incline power can also be the power gained from the gravity acting over the vehicle when moving downhill. The gravitational incline power, equation (10), is stated as a function of the vehicle speed.

$$P_{grav} = m_{veh}\, g \sin\theta\, v_{veh} \tag{10}$$

where *g* is the acceleration of gravity and θ is the angle of the road (Figure 1).

Alternatively, the gravitational power can also be expressed as a function of the vertical vehicle velocity (V_{veh_vert}), according to equations (11) and (12).

$$v_{veh\_vert} = v_{veh} \sin\theta \tag{11}$$

$$P_{grav} = m_{veh\_eq}\, g\, v_{veh\_vert} \tag{12}$$

The vehicle's change in altitude elevation (Δh) per time step (Δt) is used to estimate the unfiltered vertical velocity (v_{veh_vert}), as per equation (13)

$$v_{veh\_vert} \approx \frac{\Delta h}{\Delta t} = \frac{altitude(k) - altitude(k-1)}{\Delta t} \tag{13}$$

where *altitude*(*k*) is the k^th^ time step.

The Fleetcarma™ device does log altitude variation, but its accuracy is quite low because it is determined via GPS, which is such a poor method of estimating altitude that altitude accuracy is not even specified by GPS manufacturers (errors of tens of meters or more are commonly observed). Altitude is, therefore, instead determined using the GPS measured latitude and longitude in combination with a highly accurate topographic map. The altitude map data is determined using GPS Visualizer from the US Geological Survey's National Elevation Dataset (NED) [17].

Nevertheless, the altitude data provided by NED data still needs to be filtered due to discretization resulting from the data resolution and the irregular latitude and longitude update frequency of the Fleetcarma™ GPS device. Thus, the raw altitude data is first resampled to 1 Hz, and then a low pass Butterworth filter is applied, resulting in the filtered altitude shown in Figure 2(a) for a drive from Buffalo-NY to Hamilton-ON. To demonstrate the importance of filtering,

FIGURE 2 Altitude (a) and vertical velocity (b) calculated from NED data for one of Buffalo-NY to Hamilton-ON drive trips.

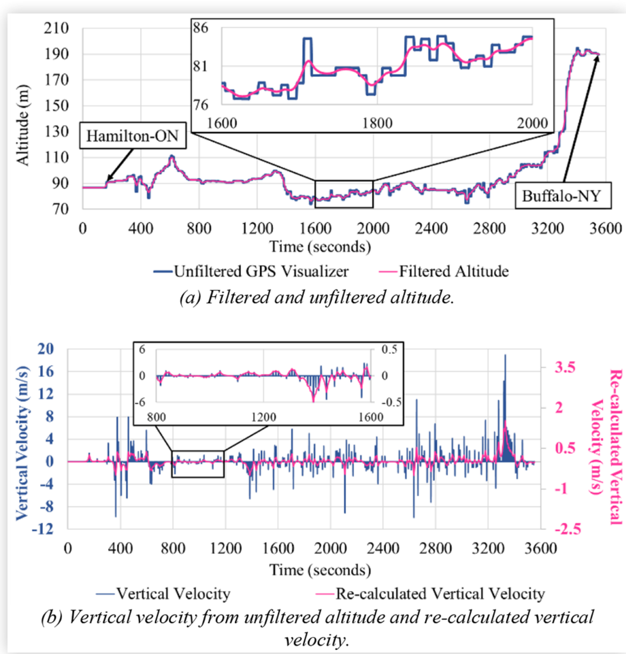

(a) Filtered and unfiltered altitude.

(b) Vertical velocity from unfiltered altitude and re-calculated vertical velocity.

the vertical velocity is calculated with filtered and unfiltered altitude and plotted in Figure 2(b).

Aerodynamic and Frictional Drag Power The frictional drag forces acting on the vehicle comprise of the aerodynamic, electric machine friction and windage, gearbox and differential friction, and bearings and tires friction. The product of the sum of all these forces, F_{drag}, and the vehicle speed defines the drag power (P_{drag}), as identified in Figure 1 and equation (14).

$$P_{drag} = F_{drag}\, v_{veh} \tag{14}$$

Typically, the drag force is estimated from a coast-down test, in which the vehicle is accelerated until a constant speed, and then it freely coasts down until a full stop. Then, from the vehicle measured coast-down deceleration rate, velocity, and mass, the drag force can be calculated and fit to a second-order polynomial equation as described in SAE J1263 [16]. The polynomial coefficients are typically referred to as the ABC parameters and are used to calculate force as defined by equation (15)

$$F_{drag} = A + Bv_{veh} + Cv_{veh}^2 \tag{15}$$

where the factor A predominantly includes tire rolling resistance, factor B comprises other speed-dependent frictional forces such as from bearings and gears, and factor C primarily captures the aerodynamic drag resistance.

The impact of the outside air temperature, T, variation is also incorporated in the model. When T increases, the C factor proportionally decreases because of the decrease of the air density. The air density is simplified to the dry air density, ρ_{dry_air}, following equation (16), and equation (17) defines the C factor.

$$\rho_{dry\_air} = \frac{P_{atmospheric}}{R_{specific}\left(T + 273.15°\text{C}\right)} \tag{16}$$

$$C \approx \frac{1}{2}\rho_{dry\_air}\, C_d\, A_{area\_veh} \tag{17}$$

where $P_{atmospheric}$ is the atmospheric pressure, $R_{specific}$ is the specific gas constant, C_d is the vehicle aerodynamic drag coefficient and A_{area_veh} is the front area of the vehicle. By substituting (16) into (17), it can be seen that C varies linearly with temperature. The measured C factor, as specified in Table 2, is determined for the temperature of 20 °C per SAE J1263, and the adjusted temperature corrected C factor can therefore be calculated using (18).

$$C_{adjusted} = C\frac{\left(20°\text{C} + 273.15°\text{C}\right)}{\left(T + 273.15°\text{C}\right)} \tag{18}$$

The temperature-adjusted $\boldsymbol{C_{adjusted}}$ factor is used in the model, allowing the model to capture the impact of temperature on aerodynamic drag forces.

Electromechanical Model

The Chevrolet Bolt EV electric traction system comprises a high-voltage (HV) battery pack, 12V accessory systems, HV to 12V DC-DC converter, as well as the traction machine DC-AC inverter and the co-axial drive unit, containing the permanent magnet synchronous machine (PMSM), single-speed gearbox, and differential, as illustrated in Figure 3. A traction system model is developed, which includes an efficiency map for the inverter and the electric machine, as well as a fixed value of 200 W for the 12V accessory system power, which is based off the measured high-voltage battery power when the vehicle is stopped. The model is not used to calculate range, only energy consumption from the battery, and it is not battery voltage-dependent, so a battery model is not included.

The modelling additionally accounts for the heater and air conditioner power, but this is based purely on the measured values during the actual drive cycles, and a model is not included. However, a model could easily be created from the measured heater and air conditioner values presented in Figure 10.

Electric Machine Model The Chevrolet Bolt EV electric machine design, speed-torque operational profile and characteristics are described in [18]. The electric machine has a peak efficiency of 97% and a continuous torque rating of approximately 60-70% of the peak torque. Table 3 summarizes the characteristics of the electric machine, and Figure 4

FIGURE 3 Chevrolet Bolt EV electromechanical schematic: energy storage system, low-voltage system, and co-axial drive unit.

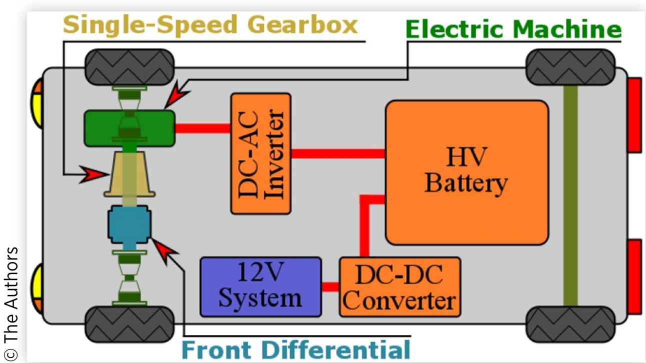

FIGURE 4 Chevrolet Bolt EV electric machine efficiency map as a function of torque and speed [18].

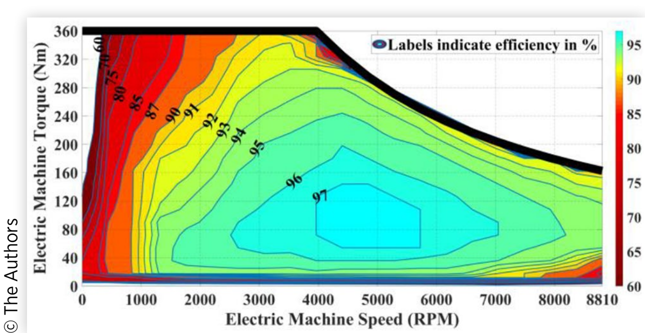

displays the measured electric machine efficiency map from [18].

The traction machine's electrical power (P_{em_elect}) is the sum of the mechanical power (P_{em_mech}) and the machine power losses (P_{em_loss}), as expressed in equation (19).

$$P_{em\_elec} = P_{em\_mech} + P_{em\_loss} \tag{19}$$

The electric machine mechanical output shaft power (P_{em_mech}) is equal to the model calculated total mechanical power (P_{mech}) and to the product of the electric machine torque (T_{em}) and speed in radians per second (ω_{em}) as shown in equation 20.

$$P_{mech} = P_{em\_mech} = T_{em}\omega_{em} \tag{20}$$

The electric machine speed in radians per second (ω_{em}) can be calculated from the vehicle speed, gear ratio, and wheel radius as in equation (21) and the speed in RPM (N_{em}) can be calculated via (22).

$$\omega_{em} = \frac{v_{veh} G_f}{r_{wh}} \tag{21}$$

$$N_{em} = \frac{60}{2\pi}\omega_{em} \tag{22}$$

The electric machine (P_{em_loss}) loss is calculated as a function of electric machine speed and torque using efficiency (η_{em}) from Figure 4, and as shown in equation (23) for both the motoring and generating cases.

$$P_{em\_loss} = \begin{cases} T_{em}\dfrac{\pi\, N_{em}}{30}\dfrac{(1-\eta_{em})}{\eta_{em}}, \textit{for motoring} \\ T_{em}\dfrac{\pi\, N_{em}}{30}(1-\eta_{em}), \textit{for generating} \end{cases} \tag{23}$$

High-Voltage DC-AC Inverter Motor Controller Model While measured efficiency values are available in the published literature for the Chevrolet Bolt EV electric machine, they are not available for the inverter. Rather than simply assuming a fixed efficiency, inverter losses, P_{inv_loss}, are instead calculated based off an IGBT semiconductor module sized appropriately for the Chevrolet Bolt EV and with phase current values for a machine with similar ratings as is described in [10]. Specifically, the loss is calculated for the Semikron Skim 909GD066HD 600 V, 900 A peak rated IGBT module, assuming 350 V dc bus voltage and fixed 40 °C heat sink temperature and the same modelling method as in [19]. The calculated efficiency map is plotted in Figure 5, showing that the peak inverter efficiency of 98% is somewhat higher than the peak efficiency of the electric machine.

FIGURE 5 Inverter efficiency map assumed for this study, calculated based off Semikron module and IPM machine with similar torque, speed, and phase current ratings.

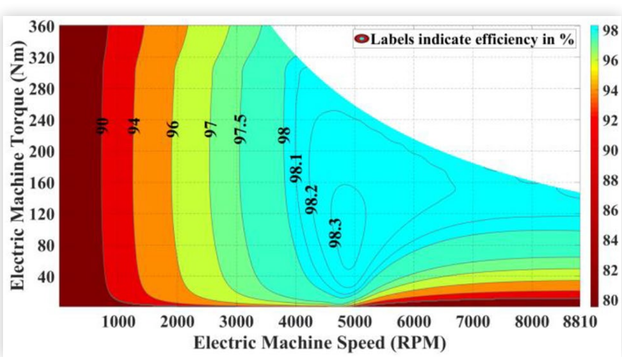

Analysis of Drive Data Logged with the Vehicle

Ninety-three drive trips, totalling 10,656.1 kilometres, were performed. The drives are primarily between Buffalo-NY, the home city of one of the coauthors, and Hamilton-ON, the location of McMaster University. All the drives are just regular trips commuting to and from work or for other personal purposes and are therefore quite representative of real-world use of the vehicle. The drives were performed under a variety of conditions, including outside air temperature from −8 to 32 °C and an approximately 128 m in elevation change for the Buffalo to Hamilton drives, as demonstrated in Figure 6. Although the altitude profile has some abrupt altitude variations due to driving on a bridge, for example, a filter has been applied to smooth these sharp variations, as previously explained.

Portions of the drives, which are more representative of city driving, less than 50 km/h, account for 30% of the total driving, whereas the remaining driving is over 50 km/h and is more representative of highway driving. Figure 7 illustrates the proportion of drive time for different logged vehicle speed ranges. The average moving speed was 70 km/h, and the maximum speed was 124 km/h.

The battery state-of-charge (SOC) at the beginning and end of each one of the 93 drives were different, as demonstrated in Figure 8. Although the SOC has a minor impact on the energy consumption (lower battery voltage may reduce inverter semiconductor switching loss, for example), SOC is

FIGURE 6 Chevrolet Bolt EV GPS logged route from Buffalo-NY to Hamilton-ON and vice-versa [20], including the Google Earth altitude variation profile.

FIGURE 7 Proportion of drive time for different logged vehicle speed ranges.

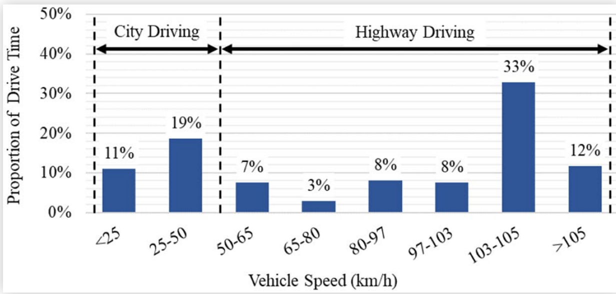

FIGURE 8 Initial and final state-of-charge (SOC) for each of the 93 drive trips from Buffalo-NY and Hamilton-ON, and vice-versa.

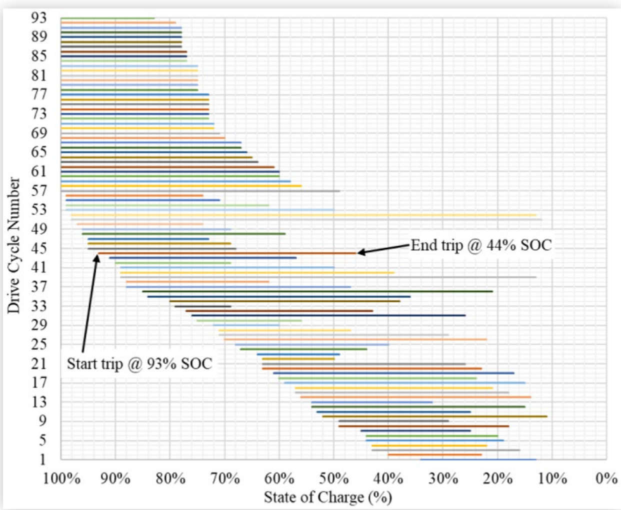

FIGURE 9 Proportion of drive time per battery power consumption.

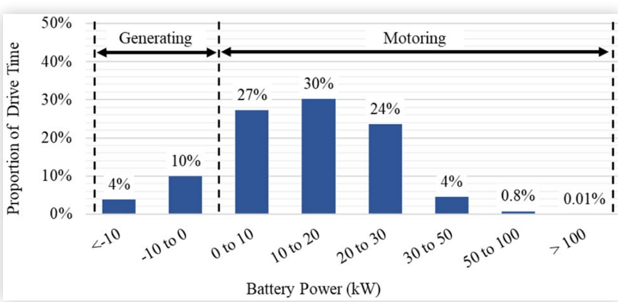

not considered in the modeling. About 1/3 of the drives started with the battery fully charged, and about 1/5 of the drives started at 60% SOC or less. At the end of the drives, the SOC was usually greater than 40%, but around 1/10 of the drives finished with a very low SOC below 15%.

The proportion of drive time per battery power range is displayed in Figure 9. The logged data shows that battery power is negative due to regenerative braking for 14% of the total drive time. For the vast majority of the time, around 80%, the electric machine is acting as a motor and battery

FIGURE 10 Average measured heater and air conditioning power demand as a function of the average outside air temperature. Drives where the heater and air conditioning power are zero, are not included.

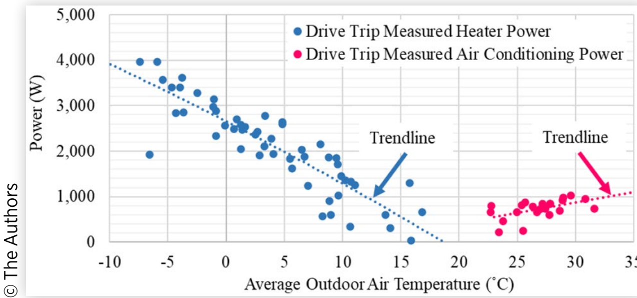

power is between positive 0 and 30 kW, showing that higher traction system power is rarely needed during typical driving. The total measured battery energy power consumed for motoring was 2,071.6 kWh and –158.8 kWh for generating.

The logged heater and air conditioning power as a function of the average outside temperature are displayed in Figure 10. As expected, the heater draws more battery power in lower temperatures and trends to zero around 18 °C (cabin temperature was typically set to around 20 °C), whereas air conditioning is utilized for temperatures above 22 °C. The average heater power demand was 2.1 kW, while the average air conditioning power demand was 0.73 kW. Regarding the total energy consumption, the heater consumed 195.2 kWh, and the air conditioning consumed 22.4 kWh. The heater energy consumption was almost nine times higher than the air conditioning energy consumption when these systems were required.

Table 4 summarizes the Chevrolet Bolt EV measured cumulative performance for all measured drive trips.

Model-Predicted Division of Energy Consumption for Logged Drives

The vehicle modelling methodology, as well as the logged data presented in the previous sections, are now applied to predict the energy consumption of the Chevrolet Bolt EV. The equation-based model was implemented in a MATLAB script. For each of the 93 drives, the model predicted mechanical frictional drag power (P_{drag}), gravitational power (P_{grav}), electric machine loss (P_{em_loss}), and inverter loss (P_{inv_loss}) were calculated at each time step and integrated to determine the total energy for each. The assumed 12V accessory power (P_{acc}, $200W$), measured heater (P_{heater}) and air conditioning (P_{air_cond}) power were likewise integrated to determine the energy for each drive cycle as well. The energy for each of these categories is then calculated as a percentage of total energy and presented in Figure 11 for drives where the heater is on, in Figure 12 for drives where the air conditioning is on, and in Figure 13 for drives where neither the heater nor the air conditioning is on.

FIGURE 11 Average distribution of system energy for the 54 Chevrolet Bolt EV drives having the **heater on** and **air conditioning off**.

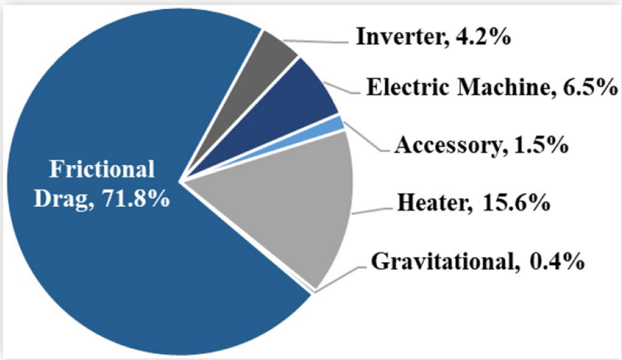

FIGURE 12 Average distribution of system energy for the 22 Chevrolet Bolt EV drives having the **heater off** and **air conditioning on**.

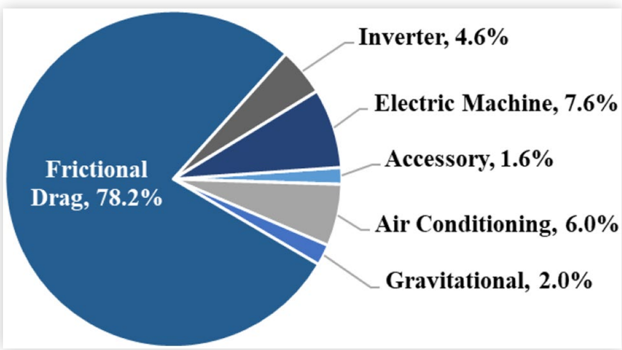

FIGURE 13 Average distribution of system energy for the 17 Chevrolet Bolt EV drives having the **heater off** and **air conditioning off**.

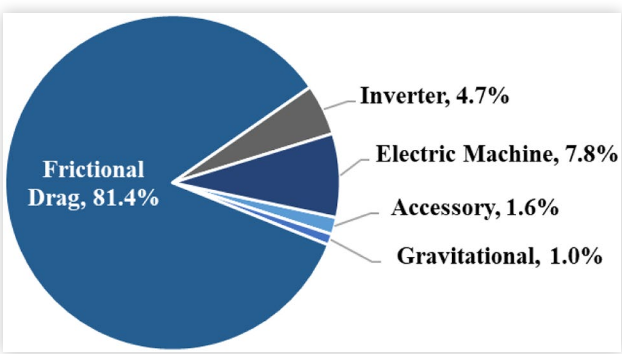

For the logged drives, the majority of the energy is used to overcome the frictional drag resistance (around 70% to 80%), followed by electric machine and inverter loss (around 12%). When the heater is on, the energy demand for this system is much higher than the consumed by the air conditioning system, nearly 16% of the total energy compared to 6% for air conditioning. If the vehicle were to use a heat pump rather than a resistive heater, the heating energy could be reduced by half or more. The potential gravitational energy to overcome up and down inclines is accountable for about 1% of the total energy on average, indicating that the analyzed trips end at a higher elevation more often than at a lower elevation.

Model Performance and Accuracy EPA Range Calculation and for Logged Drives

One way of validating the model is to compare the model estimated and manufacturer stated EPA range. The EPA cycle range for EVs is defined based on energy consumption weighted for 55% city driving (UDDS cycle) and 45% highway driving (HWFET cycle), and then scaled by a factor of 0.7 to adjust these cycles to better reflect real-world conditions [21] General Motors states an EPA range of 383 km [22] on the window label for the 2017 Chevrolet Bolt EV, which has nominal battery energy of 60 kWh [13]. The model predicts a combined weighted and scaled city/highway energy consumption of 158 Wh/km, and therefore, a total range of 380 km for the given battery nominal energy. Hence, compared to the EPA total range, the model error is just 3 km or 0.8%.

Accurate prediction of the vehicle energy consumption for the logged drives cycles is quite a bit more challenging because not all of the weather conditions, such as the impact of wind or wet or snowy roads, nor the impacts of temperature on vehicle components can be accounted for. Nevertheless, the vehicle model demonstrates fairly good accuracy, as revealed in Figure 14 and Figure 15, which compare the measured and modelled energy consumption and the error between the two as a function of the average outside temperature. Measured energy consumption is calculated from the measured battery current and voltage, while modelled energy consumption is calculated from equation 2.

The model error is between ±10% for most drive cycles below 20 °C, while the error increases significantly beyond 20 °C, with the drives typically consuming 10 to 20% less energy than predicted by the model. Overall, the error tends to underpredict energy consumption at low temperatures and overpredict energy consumption at high temperatures. There are several factors that likely contribute to this phenomenon.

FIGURE 14 Comparison of the Chevrolet Bolt EV energy consumption from measured and predicted drive trips.

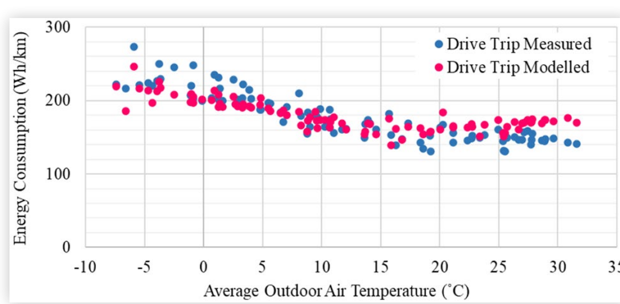

FIGURE 15 Measured versus modelled energy consumption error.

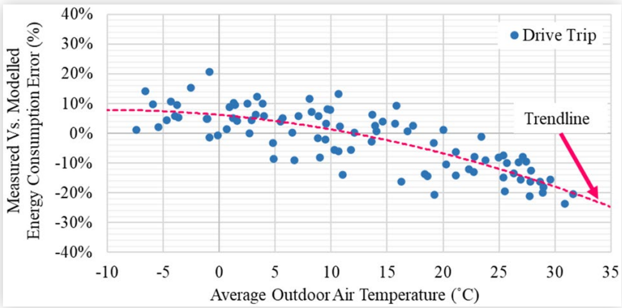

Firstly, at low temperatures, tire pressure will tend to be lower due to the lower density of air, causing more tire loss, and at higher temperatures, pressure will tend to be higher, reducing tire loss. This is not accounted for in the model but would be reflected in the ***A*** and ***B*** factors of the road load calculation. Secondly, the bearing and gear loss are also higher at low temperatures and lesser at higher temperatures, which would be reflected primarily in ***B*** factor of the road load calculation. Thirdly, the heater and air conditioning measured power values only update every 10 to 20 seconds, unlike the other measured parameters, which update every second, meaning the measured heating and air conditioning energy values may not be that accurate, further increasing error at high and low temperatures.

The average electric machine efficiency over a drive cycle, η_{em-avg}, can be calculated as in equation (25).

$$\eta_{em-avg} = \frac{\int P_{em-mech}}{\int P_{em-mech} + P_{em-loss}} \tag{25}$$

Importantly, this efficiency equation only considers net positive mechanical power to be useful output power because any negative regenerative energy will cancel out an equal amount of positive motoring energy. This effectively accounts for the roundtrip efficiency of the electric machine during regenerative braking.

The electric machine average efficiency as a function of the average vehicle speed is displayed in Figure 16. The average model predicted efficiency for all 93 drives is 92.7%, and efficiency is higher at greater speeds because the electric machine operates in a better efficiency region, as demonstrated in Figure 4.

FIGURE 16 Electric machine efficiency as a function of the average driving speed.

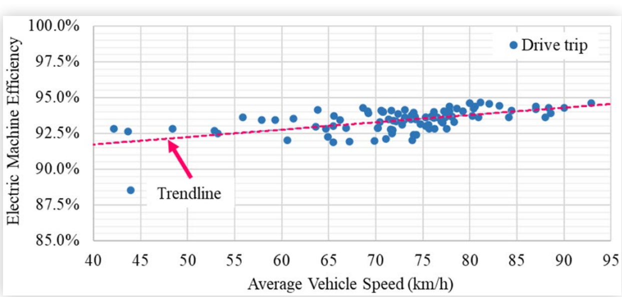

FIGURE 17 Proportion of drive time for different operational regions of modelled electric machine efficiency.

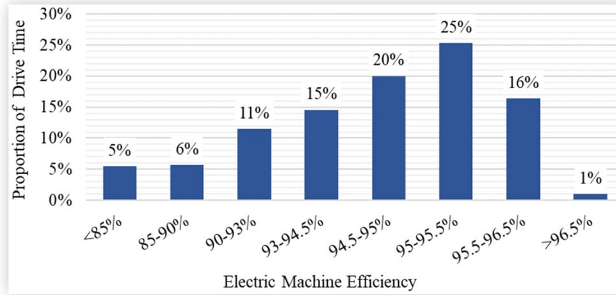

Figure 17 shows the proportion of drive time, for all 93 drives, spent at different electric machine efficiency values. The electric machine efficiency is greater than 93% for over three-quarters of the time, demonstrating it is well matched to the operating conditions.

Model Predicted Benefits of a Two-Speed Gearbox

Even though the Chevrolet Bolt EV showcases a powertrain optimized for very good efficiency with a single-speed gearbox, there is potential to further improve the efficiency with a multi-speed gearbox. Having multiple gear ratios available can enable the electric machine and inverter to operate in a higher efficiency region, resulting in a lower loss. To evaluate the potential benefits, the vehicle model is adjusted to include a two-speed gearbox. As noted in [23], gearbox efficiency tends to be lower as the number of gear ratios increase. Similarly, gearbox mass also increases with extra gear pairs, shafts, and other additional components, such as synchronizers and shift actuators. Therefore, a gearbox loss of 1% and an additional 15 kg of mass were added to the model to account for the two-speed gearbox. These assumptions could be improved based on further gearbox design and modelling.

To demonstrate the efficiency benefits of a second gear ratio, the electric machine efficiency map is transformed to be a function of the wheel torque and vehicle speed for each gear ratio. Subsequently, both efficiency maps are overlaid for a first gear ratio of 11.16 and a second gear ratio of 6.46, as illustrated in Figure 18. The shifting line indicates where efficiency is equal for both gear ratios. To the left of the shift line is more efficient to operate in the first gear, whereas to the right, the second gear is more efficient.

To determine the best gear ratios, a plethora of different gear ratio combinations were evaluated, and it was assumed that the vehicle always operated in the most efficient gear. To ensure the same or greater wheel torque, only first gear ratios of 7.05:1 or greater were considered, and to ensure the same or greater top speed, only second gear ratios of less than or equal to 7.05:1 were considered. The 55% UDDS, 45% HWFET

FIGURE 18 Chevrolet Bolt EV electric machine efficiency map for 1st and 2nd gears as a function of wheel torque and vehicle speed. It is more efficient to operate in 1st gear to the left of the shift line, whereas to the right, 2nd gear is more efficient. The considered final gear ratios 1 and 2 are 11.16:1 and 6.46:1, respectively.

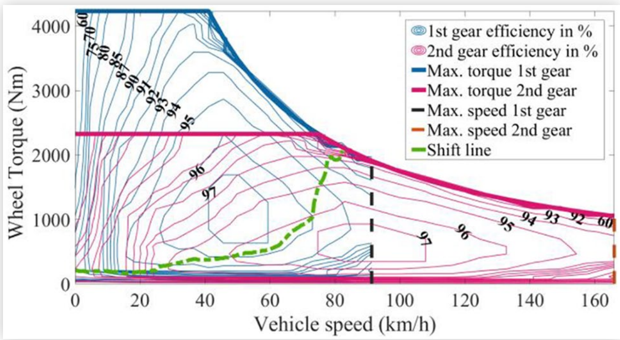

FIGURE 19 Combined electric machine and inverter average efficiency as a function of gear ratios for UDDS (55%) and HWFET (45%) drive cycle, with stock single-speed efficiency and two-gear ratio result highlighted.

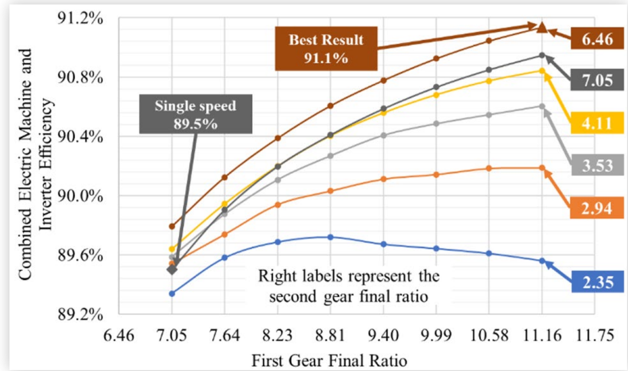

weighted average electric machine efficiency is plotted for each gear ratio combination in Figure 19.

The combined electric machine and inverter efficiency are predicted to be approximately 89.5% for the stock single-speed Chevrolet Bolt EV with a 7.05:1 gear ratio. Figure 19 also shows that as the first gear ratio increases, the efficiency of the electric machine increases due to it being able to operate in higher efficiency regions more of the time. The best case is for a first gear ratio of 11.16:1 and a second gear ratio of 6.46:1, where electric machine efficiency is 91.1%, an improvement of 1.6% compared to the single-speed vehicle. For some gear ratios, the loss is even greater, reflecting that gear ratio optimization is an important part of the design process. Additionally, a co-optimization of the electric machine, inverter and gearbox designs could result in further performance benefits.

Table 5 summarizes the difference in electric machine loss and efficiency for the two-speed and one-speed gearbox for different drive cycles. The electric machine efficiency is predicted to be improved by 2.4% for UDDS, 0.6% for HWFET, and 2.7% for US06 drive cycles, as well as up to 1.6% for the combined UDDS and HWFET. This potential efficiency improvement could be translated into a more extended drive range or a reduced battery pack for the same drive range.

The Chevrolet Bolt EV dynamic performance also benefits from the two-speed gearbox. The available torque at wheels is significantly enhanced. For instance, for the first gear ratio of 11.16:1, the maximum available wheel torque increases from 2,538 Nm to 4,018 Nm, a 58% increase. Furthermore, the maximum vehicle speed could be improved by 9%, from the predicted stock vehicle of 152 km/h to 166 km/h in the second gear with a final ratio of 6.46:1.

Conclusions

This work presented a methodology to model an electric vehicle, a 2017 Chevrolet Bolt EV, and validate it with data logged for over 10,600 km of driving. The model considers the gravitational incline power and the outside air temperature effects on the required mechanical power. The logged heater and air conditioning power demand were also integrated into

TABLE 5 Electric machine efficiency improvements achieved with a two-speed gearbox with 11.16.75:1 and 6.46:1 gear ratios.

Drive Cycle	Average Electric Machine and Inverter Energy Loss (Wh/km)	Energy Loss Reduction	Average Electric Machine and Inverter Efficiency	Average Electric Machine and Inverter Efficiency Improvement	Predicted EPA Drive Range (km)[1]	Predicted EPA Drive Range Improvement
UDDS Single-speed[2]	26.5	−18.8%	87.2%	2.4%	415	3.1%
UDDS 2-speed	21.5		89.6%		428	
HWFET Single-speed[2]	11.1	−7.2%	92.4%	0.6%	345	-0.6%
HWFET 2-speed	10.3		93.0%		343	
US06 Single-speed[2]	27.2	−27.5%	90.4%	2.7%	247	2.8%
US06 2-speed	19.7		93.0%		254	
UDDS (55%) + HWFET (45%) Single-speed[2]	19.6	−15.8%	89.5%	1.6%	380	1.3%
UDDS (55%) + HWFET (45%) 2-speed	16.5		91.1%		385	

[1] The predicted drive range is calculated based on the predicted energy consumption and scaled by a factor of 0.7.

[2] 7.05:1 gear ratio.

the model. The electromechanical model validation centred on the comparison of the measured and predicted energy consumption. The model demonstrates accuracy for real driving conditions or around ±10% for temperatures from 0 °C to 20 °C, with higher error for temperatures outside of this range. This increased error is likely due to the model not considering tire pressure variation and bearing and gear loss as a function of the outside air temperature, as well as due to lower accuracy heater and air conditioning power measurements. The model is shown to predict the EPA range of the Chevrolet Bolt EV quite well, with an error of just 3 km. Hence, the Chevrolet Bolt EV presented model provides a reasonable estimation of vehicle power and energy consumption for a given drive trip, demonstrating that a relatively simple model can be relied upon when modeling vehicle range.

Following the validation, the single-speed model of the Chevrolet Bolt EV was adapted to include a two-speed gearbox to estimate the potential benefits of such a system. With the two-speed gearbox, the electric machine and inverter combined losses were found to be reduced by 27.5% for the US06 drive cycle, which translates to an average efficiency increase of 2.7%. While this demonstrates the potential of a two-speed traction system, further investigation is needed, including gearbox loss modeling or a co-optimized design of the electric machine, inverter motor controller, battery pack and gearbox.

Future model improvements should aim to reduce the model error for temperatures below 0 °C and higher 20 °C by having more precise vehicle recorded data and accounting for more temperature-dependent loss sources. Most importantly, this paper has confirmed that EV energy consumption can be accurately estimated with relatively straightforward modeling practices, and that the proposed modelling methodology can be applied to evaluate the benefit of proposed changes and improvements to electric drivetrains, including multi-speed gearboxes, as was investigated in this study.

References

1. IEA, "Policies to Promote Electric Vehicle Deployment—Global EV Outlook 2021—Analysis," 2021, https://www.iea.org/reports/global-ev-outlook-2021/policies-to-promote-electric-vehicle-deployment.
2. General Motors, "GM's Path to an All-Electric Future," September 2021, https://www.gm.com/electric-vehicles.html.
3. Boudette, N.E. and Davenport, C., "G.M. Will Sell Only Zero-Emission Vehicles by 2035—The New York Times," 2021, https://www.nytimes.com/2021/01/28/business/gm-zero-emission-vehicles.htmlhttps://www.nytimes.com/2021/01/28/business/gm-zero-emission-vehicles.html.
4. Zhu, D., Pritchard, E.G.D., and Silverberg, L.M., "A New System Development Framework Driven by a Model-Based Testing Approach Bridged by Information Flow," *IEEE Systems Journal* 12, no. 3 (2018): 2917-2924, doi:10.1109/JSYST.2016.2631142.
5. Tran, M.-K., Akinsanya, M., Panchal, S., Fraser, R. et al., "Design of a Hybrid Electric Vehicle Powertrain for Performance Optimization Considering Various Powertrain Components and Configurations," *Vehicles* 3, no. 1 (2020): 20-32, doi:10.3390/vehicles3010002.
6. Zahid, T., Xu, K., Li, W., Li, C. et al., "State of Charge Estimation for Electric Vehicle Power Battery Using Advanced Machine Learning Algorithm under Diversified Drive Cycles," *Energy* 162 (2018): 871-882, doi:10.1016/J.ENERGY.2018.08.071.
7. Ukaew, A., "Model Based System Design of Urban Fleet Electric Vehicle Conversion," in *The 10th International Conference on Automotive Engineering—SAE Technical Papers*, SAE International, 2014, doi:10.4271/2014-01-2005.
8. Kollmeyer, P.J., Juang, L.W., and Jahns, T.M., "Development of an Electromechanical Model for a Corbin Sparrow Electric Vehicle," in *2011 IEEE Vehicle Power and Propulsion Conference*, 1-8, 2011, doi:10.1109/vppc.2011.6043208.
9. Kollmeyer, P.J., Juang, L.W., and Jahns, T.M., "Evaluation of an Electromechanical Model for a Corbin Sparrow Electric Vehicle," in *2011 IEEE Vehicle Power and Propulsion Conference, VPPC 2011*, 1-6, 2011, doi:10.1109/VPPC.2011.6043200.
10. Kollmeyer, P.J., Lamb, W., Juang, L.W., McFarland, J.D. et al., "Design of an Electric Powertrain for a Ford F150 Crew Cab Truck Utilizing a Lithium Battery Pack and an Interior PM Synchronous Machine Drive," in *2012 IEEE Transportation Electrification Conference and Expo, ITEC 2012*, 2012, doi:10.1109/ITEC.2012.6243511.
11. Kollmeyer, P.J., *Development and Implementation of a Battery-Electric Light-Duty Class 2a Truck including Hybrid Energy Storage* (Madison, WI: University of Wisconsin-Madison, 2015)
12. Lee, D., Rousseau, A., and Rask, E., "Development and Validation of the Ford Focus Battery Electric Vehicle Model," in *SAE 2014 World Congress & Exhibition*, SAE International, USA, 2014, doi:10.4271/2014-01-1809.
13. Liu, J., Anwar, M., Chiang, P., Hawkins, S. et al., "Design of the Chevrolet Bolt EV Propulsion System," *SAE Int. J. Alt. Power.* 5, no. 1 (2016): 79-86, doi:10.4271/2016-01-1153.
14. "2017 Chevrolet Bolt EV Technical Specifications," 2017, https://media.chevrolet.com/media/us/en/chevrolet/vehicles/bolt-ev/2017.tab1.html.
15. US EPA, "Annual Certification Data for Vehicles, Engines, and Equipment," 2021, https://www.epa.gov/compliance-and-fuel-economy-data/annual-certification-data-vehicles-engines-and-equipment.
16. SAE, "Road Load Measurement and Dynamometer Simulation Using Coastdown Techniques: SAE J1263_201003 Standard."
17. GPS Visualizer, "Assign DEM Elevation Data to Coordinates," October 2021, https://www.gpsvisualizer.com/elevation.
18. Momen, F., Rahman, K.M., Son, Y., and Savagian, P., "Electric Motor Design of General Motors' Chevrolet Bolt Electric Vehicle," *SAE Int. J. Alt. Power.* 5, no. 2 (2016): 286-293, doi:10.4271/2016-01-1228.
19. Allca-Pekarovic, A., Kollmeyer, P.J., Mahvelatishamsabadi, P., Mirfakhrai, T. et al., "Comparison of IGBT and SiC Inverter Loss for 400V and 800V DC Bus Electric Vehicle Drivetrains," in *2020 IEEE Energy Conversion Congress and Exposition (ECCE)*, IEEE, Detroit, MI, 6338-6344, 2020, doi:10.1109/ECCE44975.2020.9236202.

20. Google Maps, "Hamilton, ON to Buffalo, NY, USA—Google Maps," 2021, https://www.google.ca/maps/dir/Buffalo,+NY,+USA/McMaster+Automotive+Resource+Centre+(MARC),+200+Longwood+Rd+S,+Hamilton,+ON+L8P+0A6,+Canada/@43.0605213,-79.450904,67946m/data=!3m2!1e3!5s0x882c9b44784bcac3:0xdb56392cae2ee891!4m19!4m18!1m10!1m1!1s0x89d31261.

21. Good, D., *EPA Test Procedures for Electric Vehicles and Plug-In Hybrids* (Environmental Protection Agency, 2017)

22. Fuel Economy, "2017 Chevrolet Bolt EV Fuel Economy," October 2021, https://www.fueleconomy.gov/feg/Find.do?action=sbs&id=38187.

23. Naunheimer, H., Bertsche, B., Ryborz, J., and Novak, W., *Automotive Transmissions: Fundamentals, Selection, Design and Application*, 2nd ed. (New York: Springer, 2011), doi:10.1017/CBO9781107415324.004

Contact Information

Fabricio Machado
McMaster University
machadof@mcmaster.ca

Dr. Phillip Kollmeyer
McMaster University
kollmeyp@mcmaster.ca

Dr. Ali Emadi
McMaster University
emadi@mcmaster.ca

Acknowledgments

The authors would like to acknowledge Professor Jennifer Bauman of McMaster University and FleetCarma, part of Geotab Inc., for providing the data logger used for this work. Additionally, the 2017 Chevrolet Bolt EV used for this study was author Phillip Kollmeyer's personal vehicle; he received no compensation for its use in this study.

ISSN 0148-7191